Improving the Capabilities of Ultrasonic Inspection of Railroad Rails in High-Speed and Walking-Speed Testing

ALI ZARE HOSSEINZADEH, CHENGYANG HUANG, IZABELA BATISTA and FRANCESCO LANZA DI SCALEA

ABSTRACT

Ultrasonic testing is widely used to probe railroad rails for internal defects. Rails are continuously inspected by hi-rail vehicles operating ultrasonic Rolling Search Units (RSUs) at speeds up to ~30 mph. In addition, flaw detection is usually followed by flaw verification using a hand-held ultrasonic probe to determine the flaw size and orientation. Ongoing research in many laboratories worldwide is aimed at improving the performance of ultrasonic rail inspections in terms of practicality and reliability of defect detection. This paper will present recent advances on two topics: (1) achieving rail inspection at high speed by "smart trains", and (2) improving ultrasonic flaw imaging at walking speed. These efforts are being pursued at University of California San Diego (UCSD) with the collaboration of the U.S. Federal Railroad Administration (FRA) and MxV Rail, Inc. On the first topic, the latest version of a non-contact ultrasonic testing prototype will be presented to allow flaw detection at revenue speeds. Once fully developed, this capability would allow trains to perform inspections during normal operations ("smart train"), hence minimizing traffic disruptions and exploiting the redundancy of multiple train passes over the same segment of rail. Results from field tests conducted in collaboration with MxV Rail, Inc. will be presented in terms of Receiver Operating Characteristic (ROC) curves assessing the trade-off between Probability of Detection (POD) and Probability of False Alarm (PFA). On the second topic, research is being conducted to implement ultrasonic Synthetic Aperture Focus (SAF) in rail flaw imaging using a transducer array hosted in an RSU wheel. Specifically, an RSU imaging prototype is being developed based on recent advances in SAF imaging, including sparse firing, multi-mode detection and eigen-filter analysis. The latest feature allows eliminating artifacts affecting RSU rail imaging (e.g., reflections from the wheel-rail interface and from the railhead bottom flange) so as to successfully isolate the target flaws. Results will be shown during scanning of a sample rail segment in the laboratory, motivating expanding the idea for defect imaging in walking speed.

Ali Zare Hosseinzadeh; Chengyang Huang; Izabela Batista; Francesco Lanza di Scalea, Experimental Mechanics, NDE & SHM Laboratory, Department of Structural Engineering, University of California San Diego, 9500 Gilman Drive, La Jolla, CA 92093, U.S.A.

INTRODUCTION

Common rail inspection technologies, such as the Roller Search Unit (RSU), require physical contact with the rail, resulting in interruptions to the regular train service. Additionally, these technologies are limited to maximum speeds of 25 to 30 mph. To address these limitations and as an effort toward development of "smart trains," the Experimental Mechanics, NDE & SHM Laboratory at University of California San Diego (UCSD) has developed a high-speed non-contact ultrasonic testing technology for in-motion rail inspection, funded by the Federal Railroad Administration (FRA). Initiated in 2008, the UCSD team first developed an "active" laser/air-coupled system, representing the first generation of this technology [1]. This system was later refined into a "passive" air-coupled inspection system [2], which uses natural excitation waves generated by the train's wheels as the excitation source. Due to relatively low Signal-to-Noise Ratio (SNR) in tangents, the prototype was revised by incorporating a non-contact active acoustic source to enhance the excitation source energy [3, 4]. In the post-processing stage, signals acquired by two sensors (in different groups of receivers) are analyzed to extract the Green's function (or Transfer Function (TF)) for a rail segment and an outlier analysis-based technique is employed to identify discontinuity (e.g., weld, joint, or defect). The prototype is equipped with a GPS and a camera, which provides details about the prototype location and visual discontinuities (e.g., weld and joint), respectively, helping in localization and identification of the discontinuities. This paper introduces and presents the application of a segmental-averaged Normalized Cross Power Spectrum (NCPS) operator in reconstructing more robust TF. Results from field tests conducted at different speeds at Transportation Technology Center (TTC) (now MxV Rail Inc.) are presented in terms of the Receiver Operating Characteristic (ROC) curves.

The U.S. regulations mandate that when a rail flaw is detected by a hi-rail vehicle inspection system, the flaw must be manually verified. The current verification of flaws consists of a simple ultrasonic pulse-echo test conducted with a hand-held ultrasonic transducer (using a wedge) that is manually moved around the test region to attempt to estimate the flaw size and orientation (typically using a simple -6dB technique) [5]. This process yields results that are highly subjective. An improved flaw verification would allow to generate 3D images for determining the flaw size and orientation. This knowledge can inform railroad maintenance personnel for the most appropriate remedial actions. To respond to this challenge, UCSD has developed an ultrasonic Synthetic Aperture Focus (SAF)-based method for flaw imaging in rail segments using a transducer array hosted in an RSU wheel. This method benefits from sparse firing, multi-mode detection, and eigen-filter analysis to reconstruct a high-resolution image of the internal defect, while suppressing any artifacts caused by reflections from the wheel-rail interface and/or from the railhead bottom flange. This paper introduces this technology and demonstrates its application via laboratory-scale experiments.

ULTRASONIC INSPECTION OF RAILROAD RAILS IN HIGH-SPEED

This section introduces the developed technology and sensing layout for the railroad rail inspection technology in high speed. The prototype consists of various sensing layouts to collect data and track the system's accurate location during tests (see Figure 1). It

features twelve air-coupled non-contact capacitive transducers as the receivers, inclined at a 6-degree angle from the vertical to properly capture the wave leaking from the railhead to the air (according to Snell's law). A GPS unit as well as a wheel encoder are employed as positioning equipment to determine the location of the testing system while it scans the rail segments in-motion. Additionally, a laser sensor is included in the prototype to ensure proper alignment of the entire prototype with the test rail segment. A high-frame-rate GigE color camera (Basler, acA800-200gc), paired with LED lights—to optimize exposure time during image acquisition—are used as the vision sensing layout. The camera captures a lateral view of the tested rail segments, which are then used to extract ground truths, such as visible welds and joints, as well as defect locations (marked with color codes in the test farm). The processing unit includes a Real-Time (RT) Field-Programmable Gate Array (FPGA) housed in a National Instruments (NI) PXIe-1082 chassis (operated by a PXIe RT controller) and a host computer running a Windows operating system.

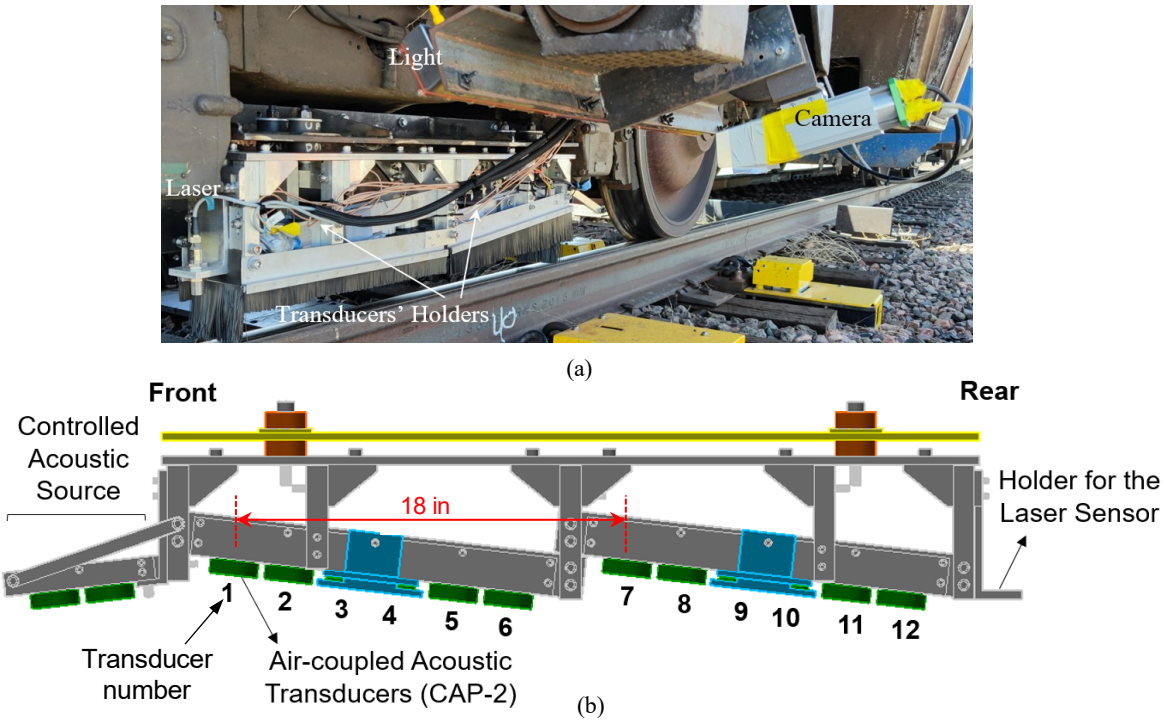

Figure 1. The high-speed rail inspection system: (a) Prototype and (b) Receivers' orientation and numbers

Two LabVIEW modules have been developed to efficiently manage data collection, transfer, and storage on the host computer for post-processing. The RT module manages data analysis on the FPGA, while the Windows module offers a user-friendly interface for controlling the data acquisition system (e.g., triggering, pausing, or stopping) and for visualizing results in real time. These two LabVIEW modules are synchronized through network communication to ensure that the data are correctly recalled and labeled according to the spatial trace of the prototype, such as the GPS coordinates.

Discontinuity Detection via Reconstructed Transfer Function: Technique and Results

The technique for high-speed rail inspection and discontinuity detection is based on reconstructing the TF between pairs of sensors. In the context of the developed prototype (shown in Figure 1), continuous excitation sources—such as the train wheels and a controlled acoustic source—launch waves into the rail, while a set of transducers collect the arriving waves. Consider two points A and B, as the receivers (for example, transducers #1 and #7, referring to Figure 1). The goal is 'robust' reconstruction of TF (or Green's function) between these two points. To achieve an accurate analogy with the ideal 'active' case (where a *virtual* pulse is applied at one point and the wave is collected at another), the TF between pairs of receivers needs to be "passively" reconstructed. The TF reconstruction between pairs of receivers is categorized as a "dual-output system" problem. Consider the frequency-domain representation of the outputs (responses) measured at points A and B shown as $O_A(\omega)$ and $O_B(\omega)$, respectively. Each of these responses are contaminated with the uncorrelated noise components, (i.e., $N_A(\omega)$ and $N_B(\omega)$). These outputs can be formulated as follows:

$$O_A(\omega) = E(\omega).EA(\omega).A(\omega) + N_A(\omega).A(\omega) \quad (1)$$

$$O_B(\omega) = E(\omega).EA(\omega).H_{AB}(\omega).B(\omega) + N_B(\omega).B(\omega) \quad (2)$$

where, $E(\omega)$, $E_A(\omega)$, and $H_{AB}(\omega)$ represent the excitation spectrum, the transfer function between source and receiver A, and the transfer function between receivers A and B, respectively. Note that the noise can originate from various sources and is assumed to be uncorrelated with the excitation. The objective here is to obtain a *pure* estimation of the transfer function $H_{AB}(\omega)$, while suppressing the effects of noise and any potential interference from the excitation.

The "deconvolution" operation is widely used in various fields to reconstruct the TF between two measurement points. However, it only provides an *estimation* of the TF, and in some cases, the SNR may be insufficient to accurately identify and track signal arrivals. To achieve a better reconstruction of the pure $H_{AB}(\omega)$, the Normalized Cross-Power Spectrum (NCPS) operator has been proposed, which is defined as a deconvolution operation implemented as the cross-power spectrum of the two receivers A and B, normalized by the auto-power spectrum of the response at receiver A [6, 7]:

$$NCPS_{A,B}(\omega) = \frac{O_A^*(\omega)O_B(\omega)}{O_A^*(\omega)O_A(\omega)} \quad (3)$$

where, * means conjugate. It is important to note that only the coherent and linear portion of the signals recorded at the location of receivers A and B are of interest for reconstructing $H_{AB}(\omega)$. Consequently, any incoherent arrivals or nonlinearities present in $N_A(\omega)$ and $N_B(\omega)$ (i.e., the noise components in $O_A(\omega)$ and $O_B(\omega)$) should be minimized as much as possible, or ideally eliminated. This is addressed by applying ensemble averaging, which effectively reduces uncorrelated noise and improves robustness for both the numerator and denominator in the NCPS metric. Therefore, the averaged-NCPS metric is formulated as:

$$NCPS_{A,B}(\omega) = \frac{\langle O_A^*(\omega) O_B(\omega) \rangle}{\langle O_A^*(\omega) O_A(\omega) \rangle} = \frac{|E(\omega)|^2 |EA(\omega)|^2 H_{AB}(\omega)}{|E(\omega)|^2 |EA(\omega)|^2 + N_A(\omega)} \quad (4)$$

It has been shown that "segmental averaging using windowed overlapping segments" can further suppress incoherent noise effects and reconstruct a more robust transfer function compared to averaging on a longer recording time window [7]. Therefore, in this study the segmental-averaged NCPS is used to reconstruct the TFs. To implement the segmental-averaged NCPS and reconstruct a robust TF, not only a suitable snapshot length, but also a suitable segment length should be considered. Assume that the optimal snapshot and segment time lengths are TL and TS, respectively, where S segments with some overlap between two successive segments (e.g., 50%) are considered. A typical snapshot is selected from the raw time history responses at the location of receivers A and B and are divided into S overlapping segments. Each time segment is zero padded and windowed and transformed to the frequency domain—using Fast Fourier Transform (FFT). The transfer function for the studied snapshot is then computed as follows [7]:

$$H_{AB}(\omega) = \frac{\sum_{i=1}^{S} O_{A,i}^*(\omega) O_{B,i}(\omega)}{\sum_{i=1}^{S} O_{A,i}^*(\omega) O_{A,i}(\omega)} \quad (5)$$

where i is the segment number. Eventually, the time-domain TF is obtained by performing an inverse FFT on $H_{AB}(\omega)$. Having TF at hand, a statistical damage index based on discontinuity-sensitive features (such as 1/variance) are combined into a feature vector and a damage index is developed based on the Mahalanobis Squared Distance metric to identify outliers as potential discontinuities [1, 3].

Figure 2 shows the results obtained from a series of field tests conducted at High-Tonnage Loop (HTL) of Transportation Technology Center (TTC) (now MxV Rail Inc.) in different speeds. The results are presented in terms of the Receiver Operating Characteristic (ROC) curves (using an inverse variance-based feature) to evaluate the trade-off between Probability of Detection (POD) and Probability of False Alarm (PFA). Also, the results are related to identifying joints and Transverse Defect (TDs). The results confirm that the segmental-averaged NCPS approach significantly enhances the SNR, particularly within the critical 100-200 μs time window (where the relevant wave arrivals for rail discontinuity detection occur). This improved SNR ensures that the primary wave packet emerges more distinctly from the noise floor, minimizing the risk of the wave packet of interest being masked by noise. Additionally, the energy becomes more concentrated within the time window of interest, while the signal tails and pre-arrivals are effectively suppressed.

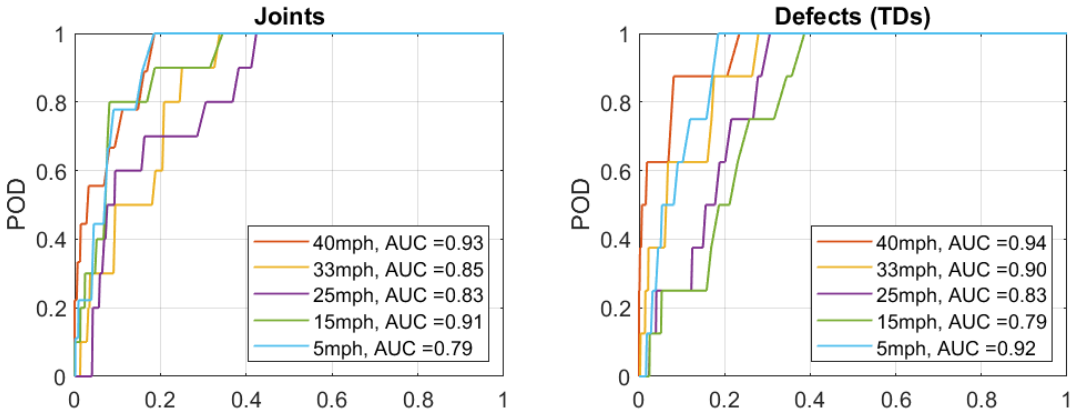

Figure 2. ROC curves for joints and transverse defect (TD) detection on the HTL track at various test speeds.

RAIL FLAW IMAGING AT WALKING SPEED

This section presents advancements in ultrasonic imaging of rail flaws using Synthetic Aperture Focus (SAF) applied with a transducer array housed in a Rolling Search Unit (RSU) wheel. The objective is to develop an in-motion, high-resolution inspection system capable of accurately detecting and sizing internal rail defects, addressing limitations in conventional pulse-echo manual inspections.

The imaging method is based on Delay-and-Sum (DAS) beamforming, enabling synthetic focusing on both transmission and reception. In the time domain, the DAS algorithm can be written as [8]:

$$I(x,y) = \sum_{i=1}^{M}\sum_{j=1}^{N} w_{ij,xy} A_{ij}\left(\tau_{ij,xy}\right) \tag{6}$$

where, $\tau_{ij,xy}$ is the time-of-flight (TOF) from transmitter i to focus point (x,y) and back to receiver j. With RSU architecture, wave propagation occurs through a water-filled tire and rail steel. Ray tracing is used to model refraction at the tire/rail interface, incorporating Snell's law and multi-mode paths including longitudinal (L) and shear (S) waves [8]. This improves imaging across a broad region-of-interest (ROI). To improve flaw detection and imaging performance, the RSU-SAFT prototype integrates: (a) sparse sub-aperture transmission to reduce scan time, (b) multi-mode detection to exploit wave-specific flaw reflections, and (c) *recursive* eigen-filter (Singular Value Decomposition (SVD) filtering) for artifact suppression. Figure 3(a) illustrates the main components in an ultrasound tomography video of the rail head. Note that when the flaw is centrally located in the ROI, the RSU image closely matches the 3D reference. However, when the defect lies ahead of the ROI, underestimation occurs due to the blind zone created by the tire/rail interface.

A key innovation in this system is the application of a recursive SVD filter to the beamformed ultrasound video data. Raw SAFT images often contain persistent clutter

resulting from wheel–rail interface reflections and structural boundaries. The recursive SVD method iteratively removes the dominant eigenmodes while maintaining positive intensity values, preserving the physical integrity of the resulting image.

Figure 3(b) presents the results of the developed imaging technique in a laboratory setting, where a rail segment containing a hole in its web was examined. The figure shows the output after applying 20 iterations of the proposed recursive SVD filter to both SS-mode and LL-mode SAFT video frames. All images are normalized using the maximum value of the Casorati matrix, which represents the highest intensity across the entire ultrasound tomography dataset. The filtered frames clearly reveal the side-drilled hole with high image quality when using the correct wave mode. A false positive appears in the alternate wave mode image, a result of beamforming with an incorrect wave velocity. However, the distinction between modes becomes visually apparent, making it feasible to isolate the correct wave mode using straightforward image segmentation techniques. Additionally, combining SS and LL images through incoherent or coherent summation can further enhance flaw contrast. In conclusion, the proposed recursive SVD filter enables accurate imaging of the flaw while effectively suppressing unwanted artifacts, such as reflections from the tire–rail interface, scattering at the rail surface, and boundary echoes from the railhead bottom. The result is a cleaner, more interpretable flaw signature in the final images.

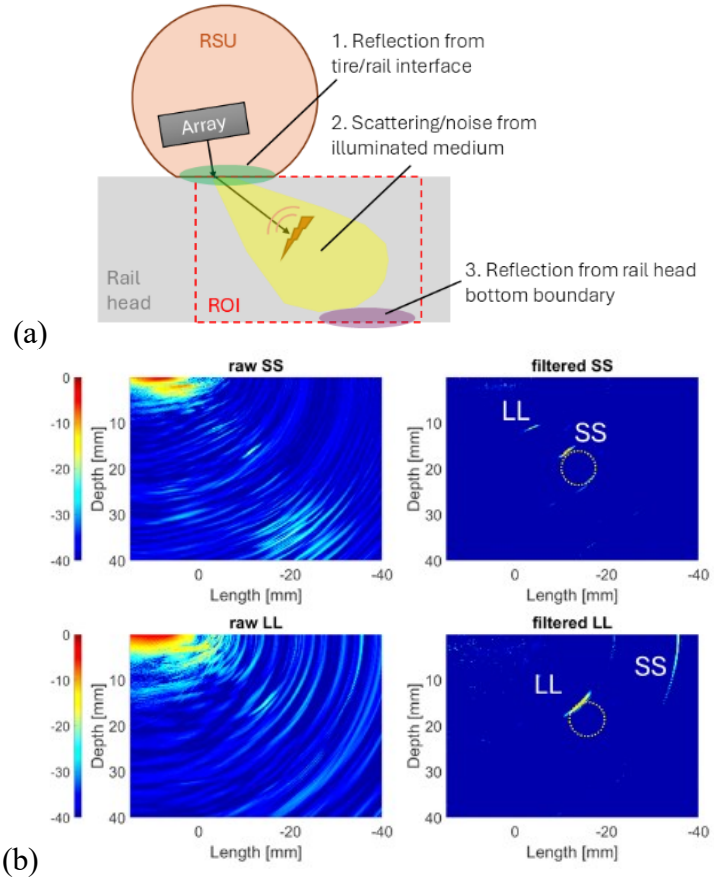

Figure 3. (a) Main components in an ultrasound tomography video of the rail head, and (b) Final output of recursive SVD filter on SS mode ultrasound video (1st row) and LL mode ultrasound video (2nd row). The hole in the rail web is shown with a dotted circle.

CONCLUSIONS

This paper presented the recent advances in high-speed rail inspection and ultrasonic flaw imaging techniques. The high-speed rail inspection is based on reconstructing the transfer function between two points of the rail using segmental-averaged Normalized Cross-Power Spectrum (NCPS) method and developing statistical approach to identify outliers as possible discontinuities. The flaw imaging method is based on ultrasonic Synthetic Aperture Focus (SAF) technique, using a transducer array hosted in a Rolling Search Units (RSU) wheel. Sparse firing, multi-mode detection and eigen-filter analysis have been employed to develop more robust imaging methods. The latest feature allows eliminating artifacts affecting RSU rail imaging, helping a successful isolation of the target flaws. The application of both methods has been demonstrated through field and laboratory-scale tests, emphasizing their promising performance in stepping toward 'smart train' concept.

ACKNOWLEDGMENT

The research works presented in this paper have received funding from the US Federal Railroad Administration (FRA) (project managers: Megan Brice and Robert Wilson) and MxV Rail, Inc (project manager: Anish Poudel).

REFERENCES

1. Mariani, S. 2015. "Non-contact Ultrasonic Guided Wave Inspection of Rails: Next Generation Approach," PhD Dissertation, University of California San Diego, La Jolla, CA, USA.
2. Lanza di Scalea, F., X. Zhu, M. Capriotti, A. Liang, and S. Mariani. 2018. "Passive Extraction of Dynamic Transfer Function from Arbitrary Ambient Excitations: Application to High-speed Rail Inspection from Wheel-generated Waves," *J. Nondestruct. Eval. Diagn. Progn. Eng. Syst.,* 1(1):011005-011005.
3. Datta, D. and F. Lanza Di Scalea. 2023. "Influence of Varying Operational Parameters on the Defect Detection Performance of a High-Speed Ultrasonic Rail Inspection System During Field Tests.," *Exp. Mech.,* 63(6):1043-1054.
4. Hosseinzadeh A. Z. and F. Lanza di Scalea. 2024. "Advanced Non-Contact Ultrasonic Monitoring System for Railroad inspection," presented at the 32nd American Society for Nondestructive Testing (ASNT) Research Symposium, Pittsburgh, PA, USA, June 24–28, 2024
5. Lanza di Scalea, F. (2007) "Ultrasonic testing applications in the railroad industry," Chapter 15: Special Applications of Ultrasonic Testing, in Non-destructive Testing Handbook, 3rd edition, P.O. Moore, ed., American Society for Nondestructive Testing, pp. 535-552.
6. Lanza di Scalea, F., S. Sternini, and A. Y. Liang. 2018. "Robust Passive Reconstruction of Dynamic Transfer Function in Dual-Output Systems," *J. Acoust. Soc. Am.,* 143(2):1019-1028.
7. Huang, C., A. Z. Hosseinzadeh, and F. Lanza di Scalea. 2024. "Ultrasparse Ultrasonic Synthetic Aperture Focus Imaging by Passive Sensing," *IEEE Trans. Ultrason. Ferroelectr. Freq. Control.,* 71(5):518-535.
8. Lanza di Scalea, F., S. Sternini, and T. V. Nguyen. 2017. "Ultrasonic Imaging in Solids Using Wave Mode Beamforming," *IEEE Trans. Ultrason. Ferroelectr. Freq. Control,* 64(3):602–616.